

## Electronic structure of metallic and semiconducting alkali-metal-lead compounds

M. Tegze\* and J. Hafner

*Institut für Theoretische Physik, Technische Universität Wien, Wiedner Hauptstrasse 8-10, A-1040 Wien, Austria*

(Received 1 December 1988)

We present an investigation of the electronic structure and the crystal binding in a number of metallic and semiconducting alkali-metal-lead compounds based on linear muffin-tin orbital calculations. We show that at all compositions the electronic structure is dominated by the strong attractive Pb potential. In compounds close to the "octet" composition  $A_4\text{Pb}$  ( $\text{Na}_{15}\text{Pb}_4\text{Li}_7\text{Pb}_2$ ) we find a narrow gap separating the nearly full occupied anion bands from the lowest cation band. However, the bonding is not truly ionic because of the strong delocalization of the lead orbital. In the equiatomic compounds containing  $\text{Pb}_4$  tetrahedra we find a gap at the Fermi level which originates from the splitting of the bands which are bonding or antibonding within the tetrahedra. However, the bonding within the  $\text{Pb}_4$  units is again not a classical covalent bond. In the Pb-rich compounds the electronic structure approaches that of pure lead.

### I. INTRODUCTION

The intermetallic phases of the alkali metals with elements of the fourth column of the Periodic System (Si, Ge, Sn, Pb) show different types of chemical bonds.<sup>1</sup> Intuitively, one would expect a predominantly ionic bond as a consequence of the large electronegativity difference between the constituent elements. The alkali-metal atom is expected to transfer its single valence electron to the group-IV element, and the most stable compound is expected at the "stoichiometric" composition  $A_4X$  ( $A$  stands for an alkali metal and  $X$  for a group-IV element) which allows for the formation of a closed octet shell. The Li-based alloy systems agree with this simple picture [Fig. 1(a) shows the Li-Pb phase diagram<sup>2</sup>]: a number of very stable crystalline compounds cluster around the "octet" composition  $\text{Li}_4\text{Pb}$ . A common feature of all these structures is that each Pb atom is surrounded by lithium atoms only. Heterocoordination is also the characteristic feature of the equiatomic compound  $\text{LiPb}$  (CsCl-type structure). No stable Pb-rich compounds are known. The phase diagrams of the Na-based alloys are quite different. In the Na-Pb system, for example<sup>3</sup> [Fig. 1(b)], we find (a) compounds close to the octet composition, such as  $\text{Na}_{15}\text{Pb}_4$ , where again each Pb atom is surrounded by Na atoms only; (b) an equiatomic compound  $\text{NaPb}$  in which tetrahedral  $\text{Pb}_4$  clusters are separated from each other by the Na atoms; and (c) a compound  $\text{NaPb}_3$  with the  $\text{Cu}_3\text{Au}$  structure, i.e., a crystal structure dominated by geometrical packing requirements. Altogether this suggests a transition from a saltlike bonding in the alkali-metal-rich regime to a largely covalent bonding at equiatomic compositions<sup>4,5</sup> (the  $\text{Pb}_4^{4-}$  clusters are isoelectronic to the tetrahedral pnictide molecules) and further to an essentially metallic bonding in the Pb-rich alloys. The phase diagrams of the heavy alkali metals K, Rb, and Cs [K-Pb is shown in Fig. 1(c)] fit into this trend:<sup>6-8</sup> there are no alkali-metal-rich compounds, the equiatomic compound  $\text{APb}$  isotopic to  $\text{NaPb}$  is very

stable, and there exists a variety of Pb-rich compounds of a largely metallic character ( $\text{KPb}_2$ , for example, is a hexagonal  $\text{MgZn}_2$ -type Laves phase).

The same structural trends are found in the liquid alloys. Diffraction experiments have shown a tendency to heterocoordination in liquid Li-Pb (Ref. 9) and Na-Pb (Refs. 10 and 11) which is strongest at the octet composition  $\text{A}_4\text{Pb}$ . It has been shown that this is well understood in terms of a strong preferential interaction between unlike atoms, and that these interatomic potentials may be derived from an electronic theory of the chemical bond. For K-Pb,<sup>11-13</sup> Rb-Pb,<sup>11</sup> and Cs-Pb,<sup>11</sup> on the other hand, the strongest ordering effects appear at the equiatomic composition. (Similar results have been reported very recently for the Sn alloys.<sup>11</sup>) It has been suggested that the tetrahedral  $\text{Pb}_4$  units characteristic of the crystalline structure are preserved in the liquid state and that the liquid structure could be considered as a random packing of  $\text{Pb}_4$  tetrahedra in a disordered alkali-metal matrix.<sup>12,13</sup> This picture has been largely confirmed by recent molecular-dynamics studies.<sup>14</sup>

The changes in the character of the chemical bond are reflected in the electronic properties of the solid and the liquid alloys. The liquid alloys have been most widely investigated.<sup>1,8</sup> In Li-Pb and Na-Pb the electrical resistivity shows sharp peaks (of the order of  $\rho \approx 500 \mu\Omega \text{ cm}$ ) and strong negative temperature coefficients of the resistivity (TCR) at the composition  $\text{A}_4\text{Pb}$ . In K-Pb, Rb-Pb, and Cs-Pb the resistivity has its maximum at the equiatomic composition ( $\rho_{\text{max}} \approx 1000 \mu\Omega \text{ cm}$  in K-Pb,  $\rho_{\text{max}} \approx 2200 \mu\Omega \text{ cm}$  in Rb-Pb, and  $\rho_{\text{max}} \approx 7000 \mu\Omega \text{ cm}$  in Cs-Pb) and the TCR's are very strongly negative. These high resistivities show that the liquid alloys are at least close to a metal-semiconductor transition and suggest that the corresponding crystalline compounds could be small-gap semiconductors. However, little is known on the electronic properties of the crystalline compounds. Resistivity measurements for amorphous Na-Sn and Cs-Sn films reported by Avci and Flynn<sup>15</sup> demonstrate the existence

of an energy gap at the equiatomic composition. Photoemission experiments confirm that CsSn is semiconducting.<sup>16</sup>

Geertsma *et al.*<sup>17,18</sup> have proposed a simplified model for the electronic structure to explain the bonding properties of the equiatomic alkali-metal—group-IV compounds. The basic assumption is that the valence states are entirely dominated by the anion states—this is a consequence of the strongly attractive anion potentials. Within a tight-binding framework the electronic Hamil-

tonian is determined by three important coupling parameters: the covalent interaction  $U$  between states of atoms within the same cluster, the intercluster transfer integral  $V$  (both  $V$  and  $U$  refer to the structure with anionic clusters), and the metallic transfer integral  $T$  relevant to a metallic structure. For this simple Hamiltonian the electronic density of states is calculated in a modified Bethe lattice approximation (each point of the Bethe lattice being occupied by an anionic cluster). Within this simple model the relative stability of the clustering and of the

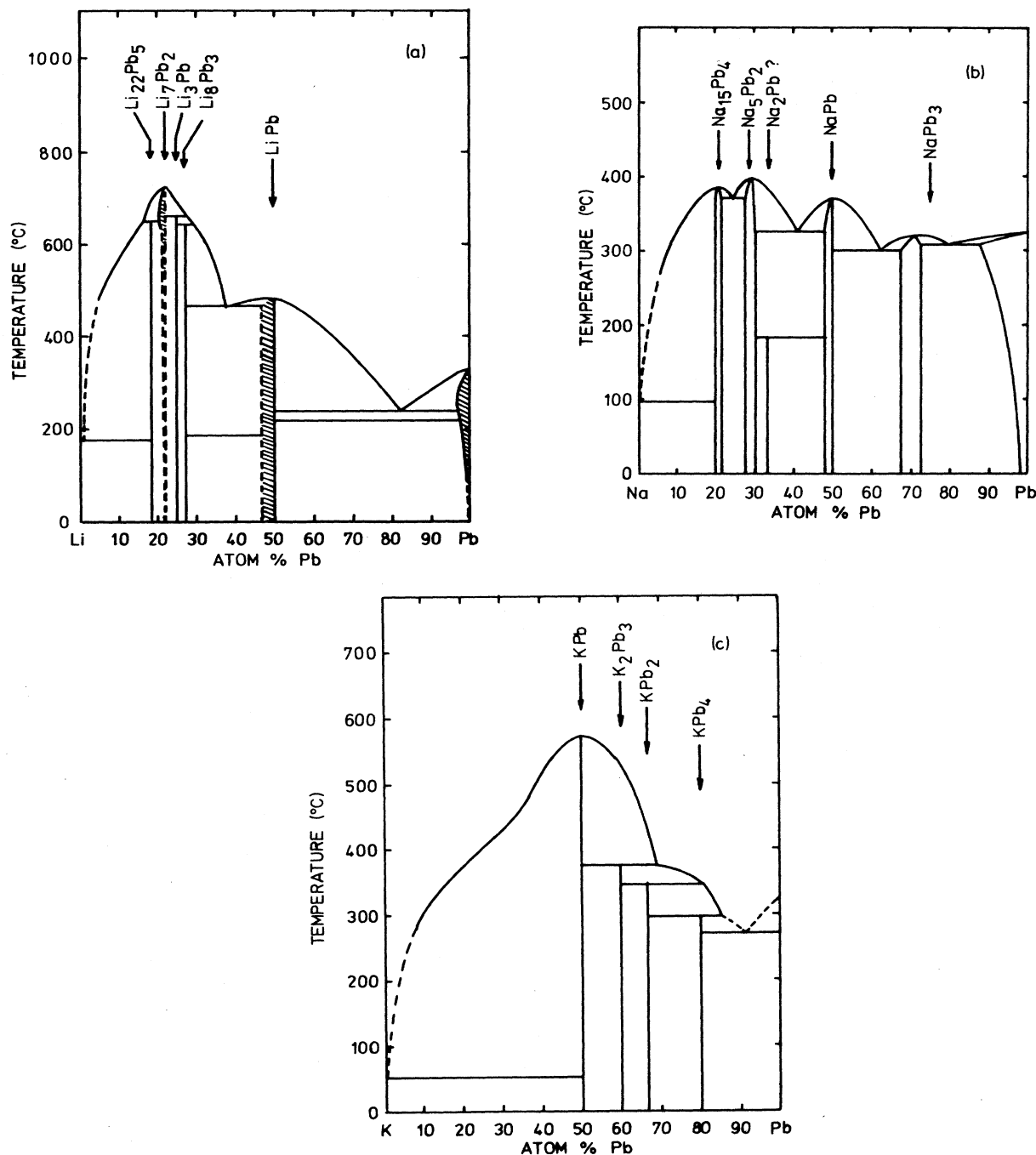


FIG. 1. Phase diagrams of (a) Li-Pb alloys (after Ref. 2), (b) Na-Pb alloys (after Ref. 3), and (c) K-Pb alloys (after Ref. 6).

metallic structures is determined by the ratio  $T/U$ . The ratio  $V/U$ , on the other hand, determines whether the covalent interaction within the cluster is strong enough to open a gap between bonding and antibonding states of the tetrahedral anionic cluster.

The essential features of this simple model have been confirmed by self-consistent calculations<sup>19</sup> of the electronic structure of NaSn (isotypic to NaPb) using the augmented-spherical-wave (ASW) method.<sup>20</sup> The density of states is shown to be dominated by the tetrahedral  $\text{Sn}_4$  units, and the Fermi level falls into the gap between the bonding and the antibonding Sn  $p$  states. The role of the Na atoms is to supply electrons for the filling of the bonding states and to keep the  $\text{Sn}_4$  tetrahedra apart, prohibiting the formation of a metallic tin band.

The aim of the present paper is to extend and to generalize the analysis of the electronic structure of alkali-metal-group-IV compounds. We present the results of self-consistent linear muffin-tin orbitals (LMTO) (Ref. 21) calculations for the intermetallic compounds  $\text{Li}_7\text{Pb}_2$ ,  $\text{LiPb}$ ,  $\text{Na}_{15}\text{Pb}_4$ ,  $\text{NaPb}$ ,  $\text{NaPb}_3$ ,  $\text{KPb}$ , and  $\text{KPb}_2$ . These compounds cover the entire range from "octet compounds" with a saltlike bonding to compounds with covalently bonded polyanionic clusters and further to metallic compounds. It is our intent to show that in all three types of compounds the electronic structure is entirely dominated by the deep anion potential and that the valence states closely resemble the anion states. In the octet compounds they are closest to the free-atom wave functions: the  $s$  states are strictly localized and only the  $p$  states interact to form a narrow band. In the cluster compounds the band picture is obtained by broadening the molecular levels of the tetrahedral  $\text{Pb}_4^{4-}$  cluster into band states. In the metallic compounds the Pb-Pb distances are nearly identical to the nearest-neighbor distances in pure Pb, and the Pb-Pb coordination numbers are of the same order of magnitude. Hence the electronic structure of these alloys is very close to that of the Pb metal. In all cases the alkali-metal atoms make no significant contribution to the electronic structure. Their role is to keep the Pb ions apart and prevent the formation of the normal Pb bands.

Our paper is organized as follows. In Sec. II we present very briefly the technical details of our calculations. Section III is devoted to the octet compounds, Sec. IV to the cluster compounds, and Sec. V to the metallic compounds. Our conclusions are given in Sec. VI.

## II. TECHNICAL DETAILS

We have used the linear muffin-tin orbitals method of Andersen *et al.*<sup>21,22</sup> in the atomic-sphere approximation (ASA). Scalar relativistic effects are included, but the spin-orbit interaction was neglected. Exchange and correlation effects are described in a local-density approximation.<sup>23</sup> The potential was calculated self-consistently. The electronic density of states was calculated using the tetrahedron method.<sup>24,25</sup> The only required input to the calculations are the positions and the atomic numbers of

the constituent elements. The radii of the atomic spheres taken as an approximation to the true Wigner-Seitz cells are calculated according to the interatomic distances in each crystal structure, except for the Li compounds and for  $\text{NaPb}_3$ . For the Li system the analysis of the variation of the excess volume with concentration suggests that the volume contraction is due to a reduction of the volume of the Li cells only. This leads to a radius ratio  $R_{\text{Li}}/R_{\text{Pb}}$  substantially smaller than 1. For  $\text{Na}_3\text{Pb}$  we used the value  $R_{\text{Na}}/R_{\text{Pb}}=1.18$  which was found to be appropriate for the other two Na-based compounds.

The most serious approximations of this approach are the use of a spherically symmetric form for the potentials, the atomic-sphere approximation to the Wigner-Seitz cell, and the local-density approximation. We feel that the ASA and the assumption of a spherically symmetric potential are well justified for most of the structures considered here, except perhaps the cluster compounds where the small number of Pb-Pb neighbors might lead to significant corrections to the muffin-tin potentials. However, these structures are so complex (64 atoms per unit cell) that we see no truly tractable alternative.

It is known from extensive studies of Ge and other small-gap semiconductors<sup>26</sup> that the effect of the local-density approximation is to make the energy gap too small. This should be kept in mind when we discuss the metal-semiconductor transition in the octet and cluster compounds.

## III. THE OCTET COMPOUNDS

In both Li-Pb and Na-Pb a large number of stable intermetallic compounds exist in a narrow range of concentration<sup>27</sup> (see Fig. 1), but no phase has the ideal stoichiometry. Not all of the structures have been completely resolved, and some of those known are prohibitively complex. For our study we have chosen the  $\text{Na}_{15}\text{Pb}_4$  and  $\text{Li}_7\text{Pb}_2$  compounds because they are closest to the octet composition and their crystal structures, albeit quite complicated, make a self-consistent calculation of the electronic structure possible. The crystal structures are quite different [ $\text{Na}_{15}\text{Pb}_4$  is body-centered cubic ( $\text{Cu}_{15}\text{Si}_4$ -type structure) with 76 atoms in the unit cell,  $\text{Li}_7\text{Pb}_2$  is hexagonal with nine atoms in the unit cell, see Table I for a full crystallographic description], but they have one thing in common: there are no Pb-Pb nearest neighbors. The shortest Pb-Pb distances are  $d_{\text{Pb-Pb}}=5.65$  Å ( $\text{Na}_{15}\text{Pb}_4$ ) and  $d_{\text{Pb-Pb}}=4.75$  Å ( $\text{Li}_7\text{Pb}_2$ ), i.e., 62% and 36% longer than the interatomic distances in pure lead.

The densities of states (DOS) calculated on a grid of 30  $\mathbf{k}$  points ( $\text{Na}_{15}\text{Pb}_4$ ) and ( $\text{Li}_7\text{Pb}_2$ ) 64  $\mathbf{k}$  points in the irreducible part of the Brillouin zone are shown in Figs. 2 and 3, respectively. Given the different crystal structures, the DOS's are surprisingly similar: a very narrow band of pure Pb  $s$  character 8 eV below the  $E_F$  containing just two electrons per lead atom, and a band about 2.5–3 eV wide just below the Fermi level (and extending slightly above it). This band contains six electrons per lead atom. It has pure  $p$  character on the Pb sites and a completely mixed character on the alkali-metal sites. This band is

separated by a very narrow gap from the first conduction band, which has predominantly *d* character on the Pb sites and again a mixed character on the alkali-metal sites.

This shows that the electronic structure is indeed dominated by the strongly attractive Pb potential. The valence-band states, in particular, all belong to the Pb atoms. This does not mean, of course, that there is a complete charge transfer from the atomic spheres centered at the alkali-metal sites to those centered at the Pb atoms. The valence charge densities are not zero or even small within the alkali-metal spheres. This means only that the valence-band states originate from the atomic Pb states, shifted and broadened by the interaction with neighboring Pb states and by the potentials of the alkali-

metal ions, but undisturbed by the alkali-metal valence states which lie well above this energy range.

Thus, even though in the octet compounds the lowest cation band is always unoccupied and separated by an "ionic" gap from the highest occupied (in our case partially occupied) anion band, their bonding cannot be considered as truly ionic. Their ionicities (calculated in terms of the net ionic charges) are always quite small due to the delocalization of the anion orbitals.

#### IV. COMPOUNDS CONTAINING POLYANIONIC CLUSTERS

The equiatomic compounds of the alkali metals except Li (Na,K,Rb,Cs) with Pb or Sn all have the same body-

TABLE I. Crystallographic description of the octet compounds  $\text{Na}_{15}\text{Pb}_4$  and  $\text{Li}_7\text{Pb}_2$ .

$\text{Na}_{15}\text{Pb}_4$ (body-centered cubic)							
Pearson symbol <i>cI</i> 76, space group $I\bar{4}3d$ , $a = 13.32 \text{ \AA}$							
Atomic positions (76 atoms/cell)							
Na <sub>1</sub>	12( <i>a</i> )		0.375	0	0.25		
Na <sub>2</sub>	48( <i>e</i> )		0.120	0.160	0.960		
Pb	16( <i>c</i> )		0.208	0.208	0.208		
Coordination							
	Na <sub>1</sub>	Na <sub>2</sub>	Pb	Na	Total		
Na <sub>1</sub>	0	8	4	8	12		
Na <sub>2</sub>	2	5(+3)	3	7(+3)	10(+3)		
Pb	3	9	0	12	12		
Interatomic distances ( $\text{\AA}$ )							
$d_{\text{Na-Na}} = 3.39\text{--}3.63$ (4.00–4.10)							
$d_{\text{Na-Pb}} = 3.26\text{--}3.60$							
Wigner-Seitz radii							
$R_{\text{Na}} = 1.9890 \text{ \AA}$ , $R_{\text{Pb}} = 1.7919 \text{ \AA}$ , $R_{\text{Na}}/R_{\text{Pb}} = 1.11$							
$\text{Li}_7\text{Pb}_2$ (hexagonal)							
Pearson symbol <i>hP</i> 9, space group <i>P</i> 321							
$a = 4.751 \text{ \AA}$ , $c = 8.589 \text{ \AA}$ , $c/a = 1.8078$							
Atomic positions (9 atoms/cell)							
Li <sub>1</sub>	1( <i>a</i> )		0	0	0		
Li <sub>2</sub>	2( <i>c</i> )		0	0	0.333		
Li <sub>3</sub>	2( <i>d</i> )		0.333	0.667	0.583		
Li <sub>4</sub>	2( <i>d</i> )		0.333	0.667	0.917		
Pb	2( <i>d</i> )		0.333	0.667	0.25		
Coordination							
	Li <sub>1</sub>	Li <sub>2</sub>	Li <sub>3</sub>	Li <sub>4</sub>	Pb	Li	Total
Li <sub>1</sub>	0	2	0	6	0(+6)	8	8(+6)
Li <sub>2</sub>	1	1	3(+3)	0(+3)	3	5(+6)	8(+6)
Li <sub>3</sub>	0	3(+3)	3	1	4	7(+3)	11(+3)
Li <sub>4</sub>	3	0(+3)	1	3	4	7(+3)	11(+3)
Pb	0(+3)	3	4	4	0	11(+3)	11(+3)
Interatomic distances ( $\text{\AA}$ )							
$d_{\text{Li-Li}} = 2.83\text{--}3.10$ (3.48)							
$d_{\text{Li-Pb}} = 2.83\text{--}3.10$ (3.48)							
Wigner-Seitz radii							
$R_{\text{Li}} = 1.5289 \text{ \AA}$ , $R_{\text{Pb}} = 1.9601 \text{ \AA}$ , $R_{\text{Li}}/R_{\text{Pb}} = 0.78$							

centered tetragonal structure with 64 atoms per unit cell<sup>4,5,28,29</sup> (see Table II for a summary of the relevant crystallographic information). This structure consists of Pb(Sn) tetrahedra, separated by the alkali-metal atoms (Fig. 4) in such a way that four alkali-metal atoms again form a large tetrahedron oriented in the opposite direction. The center of the Pb tetrahedra does not have the full tetrahedral point-group symmetry ( $T_d$ ), but the interatomic Pb-Pb distances within a tetrahedron agree nonetheless to within 2%. These distances are smaller than the nearest-neighbor distances in pure fcc Pb by 9–10% in NaPb and 2–3% in KPb. The Pb tetrahedra are arranged such as to keep Pb atoms from different tetrahedra as far apart as possible. Each Pb atom has only one next-nearest Pb neighbor at a distance of 3.64 Å in NaPb and 3.92 Å in KPb. Compared to the pure alkali metals, the Na-Na nearest-neighbor distance in NaPb is about 2% larger, while the K-K distances in KPb are about 11% smaller. This is related to a very large negative excess volume in KPb ( $\Delta V = -24\%$ ) and a much smaller one in NaPb ( $\Delta V = -9\%$ ). For a simple model for the origin of the excess volumes, see Ref. 30.

The compounds formed by (Na,K,Rb,Cs) with the lighter group-IV elements have another three different crystal structures (the NaSi, NaGe, and KGe struc-

tures).<sup>31,32</sup> All of these show the characteristic tetrahedra. Thus one is led to the conclusion that the tetrahedra of the group-IV atoms possess a rather high stability.

The densities of states (calculated on a basis of 50  $k$  points) are shown in Figs. 5 and 6. All the valence bands are again dominated by the Pb states. The  $s$  band is now split into two narrow bands, the lower one containing 0.5 and the higher one 1.5 electrons per Pb atom. Relative to the Fermi level the position of the upper part of the  $s$  band in NaPb is about the same as that of the  $s$  band in  $\text{Na}_{15}\text{Pb}_4$ . The Pb  $p$  band is equally divided into a bonding and an antibonding part, the Fermi level falling in the gap between the top of the bonding bands and the bottom of the antibonding bands. The antibonding Pb  $p$  bands overlap with the Pb  $6d$  band at about 2.5 eV. The DOS at the Na (K) sites is always similar in shape to the total DOS. As in the octet compounds we find a strong mixing of all angular momentum components, with a general trend to find more  $s$  character at the bottom and more  $p$  character at the top of each separate band. In KPb the strong contraction of the K-K nearest-neighbor distances leads to a lowering of the bottom of the K band. Thus the antibonding Pb  $p$  band overlaps not only with the Pb  $d$  band, but also with the K band.

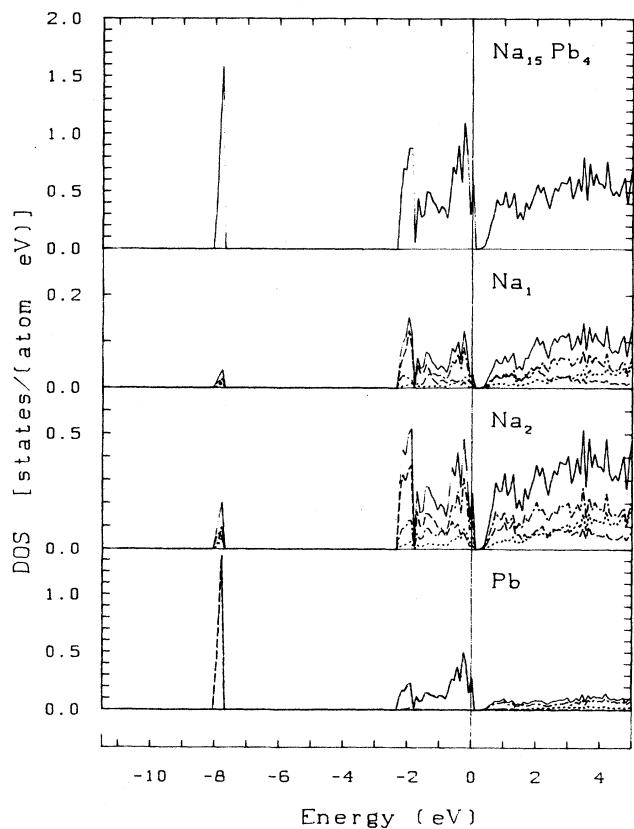


FIG. 2. Total, site-, and angular-momentum-decomposed density of states for  $\text{Na}_{15}\text{Pb}_4$ . Solid lines denote total DOS, dashed lines denote  $s$  states, dot-dashed lines denote  $p$  states, and dotted lines denote  $d$  states. The zero of the energy scale is at the Fermi level.

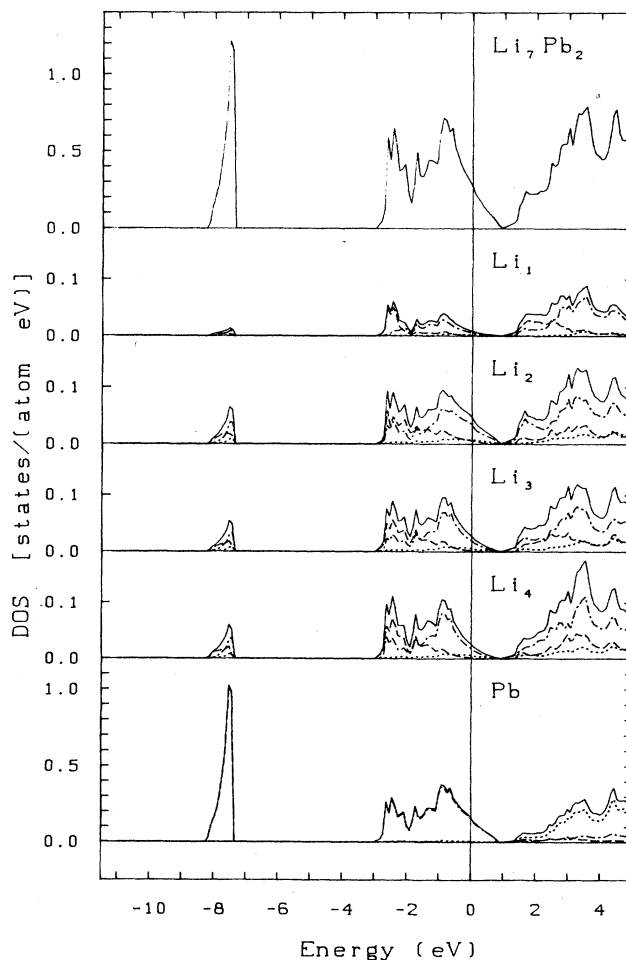


FIG. 3. Total, site-, and angular-momentum-decomposed density of states for  $\text{Li}_7\text{Pb}_2$ . Same symbols as Fig. 2.

TABLE II. Crystallographic description of the NaPb and KPb compounds.

		NaPb (body-centered tetragonal)				
		Pearson symbol $tI64$ , space group $I4_1/acd$				
NaPb	$a = 10.58 \text{ \AA}$ $c = 17.75 \text{ \AA}$ $c/a = 1.6773$				KPb	$a = 11.50 \text{ \AA}$ $c = 18.76 \text{ \AA}$ $c/a = 1.6313$
Atomic positions (64 atoms/cell)						
Na <sub>1</sub>	16( <i>e</i> )		0.25		0.125	0.125
Na <sub>2</sub>	16( <i>f</i> )		0.625		0.625	0.25
Pb	32( <i>g</i> )		0.0696		0.8686	0.0633
Coordination						
	Na <sub>1</sub>	Na <sub>2</sub>	Pb		Na	Total
Na <sub>1</sub>	0	4	8		4	12
Na <sub>2</sub>	4	1	6		5	11
Pb	4	3	3(+1)		7	10(+1)
Interatomic distances ( $\text{\AA}$ )						
$d_{\text{Na-Na}} = 3.69\text{--}3.74$					$d_{\text{K-K}} = 3.98\text{--}4.06$	
$d_{\text{Na-Pb}} = 3.39\text{--}3.62$					$d_{\text{K-Pb}} = 3.56\text{--}3.85$	
$d_{\text{Pb-Pb}} = 3.15\text{--}3.16$ (3.64)					$d_{\text{Pb-Pb}} = 3.38\text{--}3.41$ (3.92)	
Wigner-Seitz radii						
$R_{\text{Na}} = 2.0963 \text{ \AA}$					$R_{\text{K}} = 2.2575 \text{ \AA}$	
$R_{\text{Pb}} = 1.7765 \text{ \AA}$					$R_{\text{Pb}} = 1.9132 \text{ \AA}$	
$R_{\text{Na}}/R_{\text{Pb}} = 1.18$					$R_{\text{K}}/R_{\text{Pb}} = 1.18$	

Our results are very similar to those obtained by Spröngelkamp *et al.*<sup>19</sup> for  $\beta$ -NaSn and lend full support to the interpretation of the electronic structure of the NaPb-type intermetallic compounds in terms of the molecular eigenstates of  $\text{Pb}_4^{4-}$  polyanions isoelectronic to the tetrahedral pnictide molecules advocated by Geertsma *et al.*<sup>17,18</sup> The electronic spectrum of the tetrahedral pnictide molecules was investigated by Hart *et al.*<sup>33</sup> and Goodman *et al.*<sup>34</sup> In an (*s,p*) basis the 16-dimensional representation of the tetrahedron group  $T_d$  may be reduced in the following way: the *s* states reduce to the  $A_1$  and  $T_2$  irreducible representations, the *p* states to  $A_1$ ,  $E$ ,  $2T_2$ , and  $T_1$ . The actual splitting of the levels depends strongly on the values chosen for the transfer integrals, but for any reasonable assumption it is found that the *s* levels ( $A_1, T_2$ ) are always far below the *p* levels which are grouped into three bonding levels ( $E, T_2, A_1$ ) and two antibonding levels ( $T_1, T_2$ ), only the bonding levels being occupied.<sup>17,18,35</sup> In the solid these levels are broadened into bands due to the interaction among adjacent tetrahedra.

However, this should not lead to the conclusion that the  $\text{Pb}_4^{4-}$  tetrahedra are stabilized by a conventional covalent bond. Because of the rather extended nature of the Pb *p* orbitals one cannot sustain a picture of a tetrahedron stabilized by four two-electron-two-center bonds. Indeed, Hart *et al.*<sup>33</sup> have shown that in the  $P_4$  molecule the maxima of the valence-electron distribution are found above each of the triangular tetrahedron faces. The maxima arise from the overlap of three *p*-orbital lobes: the atoms occupy four corners of a cube with the electron density situated at the opposite four corners. Such a picture would also explain the structure in the partial alkali-metal DOS. The alkali-metal atoms are sit-

uated very close to the charge-density maxima. Thus the hybridized wave functions are even with respect to the Na atoms and at these energies one finds mostly Na *s* states.

## V. METALLIC COMPOUNDS

The three metallic alkali-metal-lead compounds included in our study have rather different crystal structures. LiPb has the CsCl structure, i.e., Li and Pb occupy interpenetrating simple-cubic lattices such that Pb is surrounded by Li atoms only and vice versa. NaPb<sub>3</sub> has the AuCu<sub>3</sub> structure which may be viewed as a face-centered Pb lattice where every fourth Pb atom (say those situated at the corners of the cubic unit cell) is substituted by a sodium atom. KPb<sub>2</sub> has the structure of a hexagonal

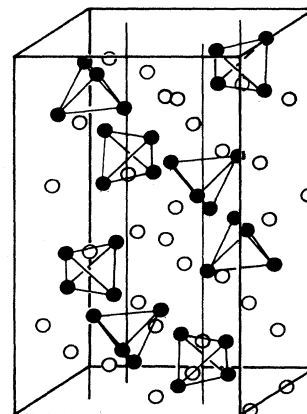


FIG. 4. The crystal structure of NaPb and KPb (after Ref. 19).

MgZn<sub>2</sub>-type Laves phase. In the KPb<sub>2</sub> structure the Pb atoms are arranged on a network of tetrahedra: two Pb tetrahedra share a triangular face, they are linked via corners to other Pb<sub>5</sub> double tetrahedra so as to form a continuous network. The K atoms are located in the large holes of this network on a wurtzite-type sublattice (Fig. 7). The crystallographic data of all three compounds are summarized in Table III.

A common feature of all three compounds is that the shortest Pb-Pb distances are close to the nearest-neighbor distances in pure lead (they are 2% larger in LiPb, 1% smaller in NaPb<sub>3</sub>, and 6% smaller in KPb<sub>2</sub>). The shortest distances between the alkali-metal ions, on the other hand, are larger than those in the pure alkali metals in LiPb (by 18%) and NaPb<sub>3</sub> (by 33%), but contracted in KPb<sub>2</sub> (by 11%). In the following we discuss the electronic structure of these compounds in the sequence of increasing Pb content.

The electronic density of states for LiPb is shown in Fig. 8. It has been calculated from a mesh of 120 *k* points. Again the Li states play only a very minor role. The total density of states is essentially that of a simple-cubic metal such as As, Sb, and Bi under elevated pressure.<sup>36</sup> Due to the large difference in the atomic-energy

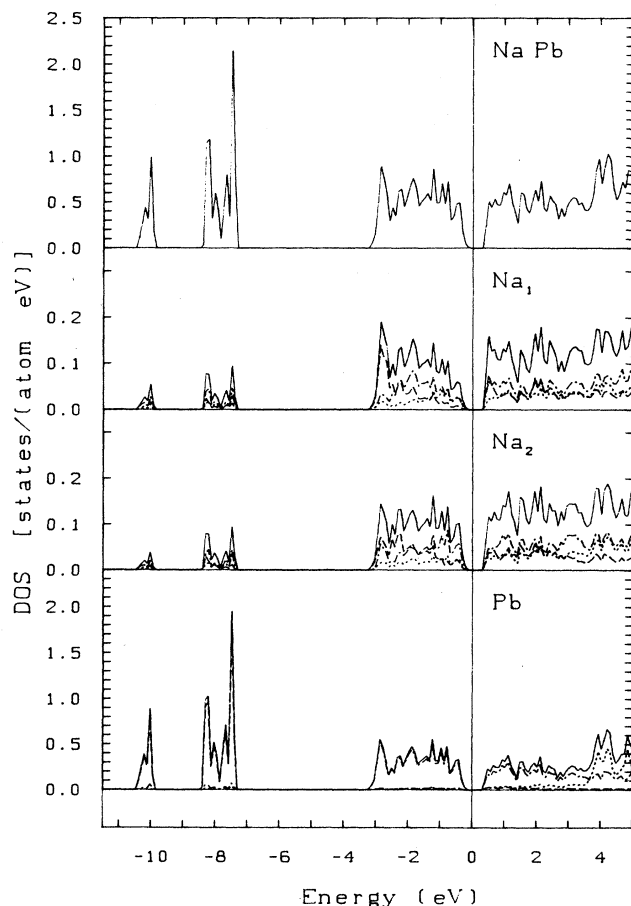


FIG. 5. Total, site-, and angular-momentum-decomposed density of states for NaPb. Same symbols as Fig. 2.

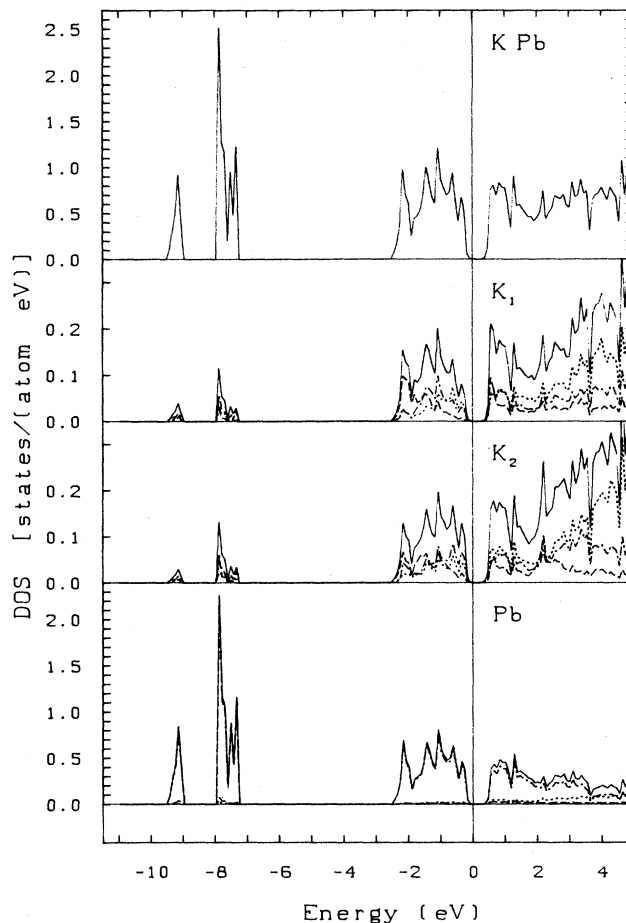


FIG. 6. Total, site-, and angular-momentum-decomposed density of states for KPb. Same symbols as Fig. 2.

eigenvalues of the *s* and *p* states, the band splits into a low-lying *s* band whose width is nearly identical to the width of the *s* band in pure lead (see, e.g., Ref. 37 and below). The band at the Fermi level is dominated by the Pb *p* states. The overlap of the lobes of the *p* states stabilizes the simple-cubic sublattice of lead. The band is ex-

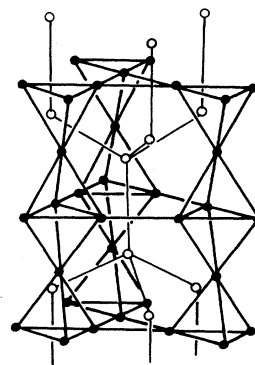


FIG. 7. The crystal structure of KPb<sub>2</sub>.

TABLE III. Crystallographic description of the LiPb, KPb<sub>2</sub>, and NaPb<sub>3</sub> compounds.

LiPb [simple-cubic (CsCl-type)]					
Pearson symbol <i>cP</i> 2, space group <i>Pm</i> $\bar{3}$ <i>m</i> , <i>a</i> = 3.563 Å					
Atomic positions (2 atoms/cell)					
Li	1( <i>a</i> )		0	0	0
Pb	1( <i>b</i> )		0.5	0.5	0.5
Coordination					
		Li		Pb	Total
Li		0(+6)		8	8(+6)
Pb		8		0(+6)	8(+6)
Interatomic distances					
$d_{\text{Li-Li}} = d_{\text{Pb-Pb}} = 3.563 \text{ \AA}$					
$d_{\text{Li-Pb}} = 3.086 \text{ \AA}$					
Wigner-Seitz radii					
$R_{\text{Li}} = 1.5147 \text{ \AA}$ , $R_{\text{Pb}} = 1.9419 \text{ \AA}$ , $R_{\text{Li}}/R_{\text{Pb}} = 0.78$					
KPb <sub>2</sub> [hexagonal (MgZn <sub>2</sub> -type)]					
Pearson symbol <i>hP</i> 12, space group <i>P</i> 6 <sub>3</sub> / <i>mmc</i> , <i>a</i> = 6.66 Å, <i>c</i> = 10.76 Å, <i>c/a</i> = 1.6156					
Atomic positions (12 atoms/cell)					
K	4( <i>f</i> )		0.333	0.667	0.063
Pb <sub>1</sub>	2( <i>a</i> )		0	0	0
Pb <sub>2</sub>	6( <i>h</i> )		0.830	0.661	0.25
Coordination					
	K	Pb <sub>1</sub>	Pb <sub>2</sub>	Pb	Total
K	4	3	9	12	16
Pb <sub>1</sub>	6	0	6	6	12
Pb <sub>2</sub>	6	2	4	6	12
Interatomic distances (Å)					
$d_{\text{K-K}} = 4.03\text{--}4.07$					
$d_{\text{K-Pb}} = 3.86\text{--}3.90$					
$d_{\text{Pb-Pb}} = 3.28\text{--}3.39$					
Wigner-Seitz radii					
$R_{\text{K}} = 2.2324 \text{ \AA}$ , $R_{\text{Pb}} = 1.8918 \text{ \AA}$ , $R_{\text{K}}/R_{\text{Pb}} = 1.18$					
NaPb <sub>3</sub> [simple-cubic (AuCu <sub>3</sub> -type)]					
Pearson symbol <i>cP</i> 4, space group <i>Pm</i> $\bar{3}$ <i>m</i> , <i>a</i> = 4.884 Å					
Atomic positions (4 atoms/cell)					
Na	1( <i>a</i> )		0	0	0
Pb	3( <i>c</i> )		0	0.5	0.5
Coordination					
	Na		Pb	Total	
Na	0		12	12	
Pb	4		8	12	
Interatomic distances					
$d_{\text{Na-Pb}} = d_{\text{Pb-Pb}} = 3.454 \text{ \AA}$					
$d_{\text{Na-Na}} = 4.884 \text{ \AA}$					
Wigner-Seitz radii					
$R_{\text{Na}} = 2.1430 \text{ \AA}$ , $R_{\text{Pb}} = 1.8161 \text{ \AA}$ , $R_{\text{Na}}/R_{\text{Pb}} = 1.18$					

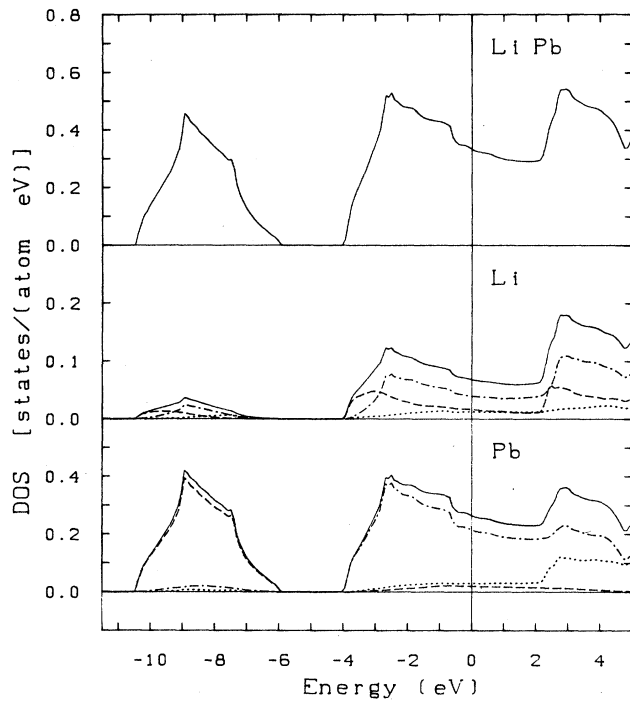


FIG. 8. Total, site-, and angular-momentum-decomposed density of states for LiPb. Same symbols as Fig. 2.

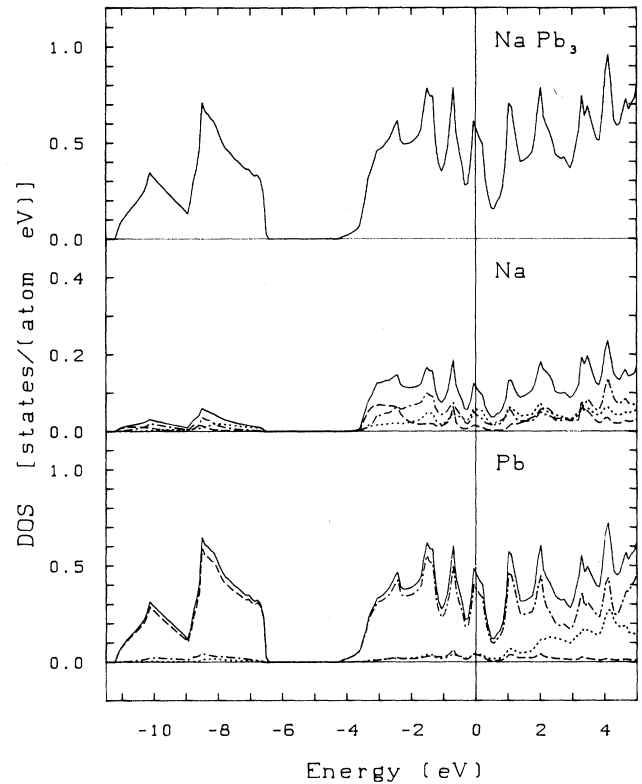


FIG. 10. Total, site-, and angular-momentum-decomposed density of states for NaPb<sub>3</sub>. Same symbols as Fig. 2.

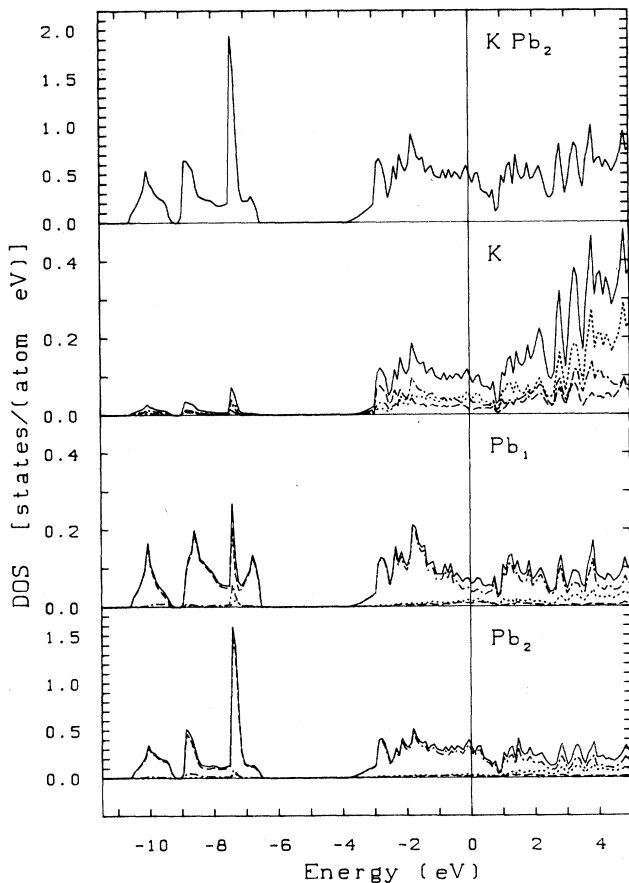


FIG. 9. Total, site-, and angular-momentum-decomposed density of states for KPb<sub>2</sub>. Same symbols as Fig. 2.

actually half-filled. This could lead to an instability against a Peierls-type distortion as in the pentavalent semimetals (As,Sb,Bi). However, the Pb-Pb distances are still metallic so that the Pb-Pb interaction is too weak to cause such an instability. The Li-DOS again has a completely mixed character, except for a slight tendency to have more *s* character at the bottom of each band and more *p* and *d* character in the middle and at the top of the band. This is due to the same mechanism as discussed above for NaPb and KPb: the hybridized Pb *p* orbitals are even

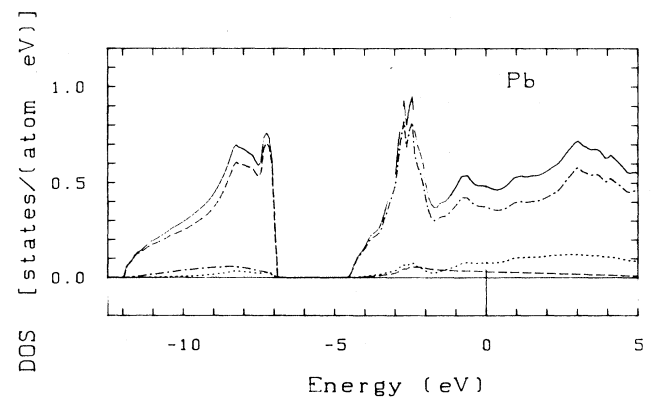


FIG. 11. Total, site-, and angular-momentum-decomposed density of states for fcc Pb. Same symbols as Fig. 2.

TABLE IV. Trends in the relevant parameters determining the electronic structure of alkali-metal-lead compounds (see text).

		Compound		
Li <sub>7</sub> Pb <sub>2</sub> Na <sub>15</sub> Pb <sub>4</sub>	LiPb NaPb KPb		NaPb <sub>3</sub>	Pb
Pb concentration				
0.22	0.5			1
0.21	0.5		0.75	
	0.5	0.67		
Number of electrons per Pb atom				
7.5	5			4
7.75	5		4.33	
	5	4.5		
Volume per Pb atom (Å <sup>3</sup> )				
84.0	45.2			30.3
147.7	62.1		38.8	
	77.5	51.7		
<i>s</i> -band width (eV)				
0.82	4.5			5.2
0.28	3.1		4.7	
	2.2	4.1		
<i>p</i> -band width (eV)				
3.9	7.9			11.8
2.4	6.5		9.8	
	5.4	8.4		

with respect to the Na sites so that their overlap is bonding with the Na *s* states.

The electronic structure of KPb<sub>2</sub> (calculated on a basis of 27 *k* points, Fig. 9) is intermediate between that of the cluster compounds and the metallic bands of LiPb, NaPb<sub>3</sub>, and pure lead. Compared to KPb, the *s* band is broadened, but the splitting into two subbands corresponding to the tetrahedral eigenstates is still clearly recognizable. The splitting of the *p* band which is the origin of the gap in the cluster compounds is reduced. Due to the connectedness of the Pb-tetrahedra states which are antibonding within a tetrahedron and bonding between the tetrahedra are lowered in energy and this closes the gap in the middle of the *p* band. All the lower bands have again a completely mixed character on the potassium sites.

The electronic DOS of NaPb<sub>3</sub> (calculated from a mesh of 120 *k* points, see Fig. 10) is very similar to that of pure fcc Pb (Fig. 11), except for some structure in both the *s* and the *p* bands which appears as a consequence of the breaking of fcc symmetry. The DOS on the sodium sites is of a mixed character over the entire energy range considered.

## VI. DISCUSSION

We have found that the electronic structure of *all* alkali-metal-lead compounds, ranging from the ionic octet compounds to the covalent-ionic cluster compounds and to the metallic Pb-rich compounds, is entirely dom-

inated by the strong attractive Pb potential. The role of the alkali-metal atoms is to keep the Pb atoms apart and to provide a "bridging" function between the Pb atoms or clusters. This is illustrated in Table IV and Fig. 12. This figure shows the total DOS of all compounds arranged according to the volume available per lead atom. In the octet compounds this volume is very large. Thus we find relatively narrow bands derived from the energy eigenvalues of the free Pb atom. The Pb bands are separated by a very narrow ionic gap from the lowest unoccupied cation band. Due to the large overlap of the Pb orbitals into the alkali-metal spheres, ionicities defined in terms of net ionic charges are very small, so that the bonding cannot be truly termed ionic.

As the volume per lead atom decreases, the overlap between the Pb states becomes strong enough to stabilize isolated anionic clusters. The electronic structure is determined by the molecular eigenvalues of these clusters. A "covalent" gap separates the Pb *p* bands which are bonding within such a cluster from those which are antibonding within such a cluster. This explains the unusual electronic transport properties of NaPb and KPb. Again the role of the alkali-metal atoms is to keep these clusters apart and to provide some weak bridging bonds. On the other hand, it is also important—as stressed by Springelkamp *et al.*<sup>19</sup>—that the Pb clusters keep the alkali-metal atoms apart to prevent a lowering of the alkali-metal band below the Fermi level. Again the delocalization of the Pb states does not allow us to consider the bonding within the Pb<sub>4</sub><sup>4-</sup> clusters as truly covalent in the sense of localized two-electron bonds.

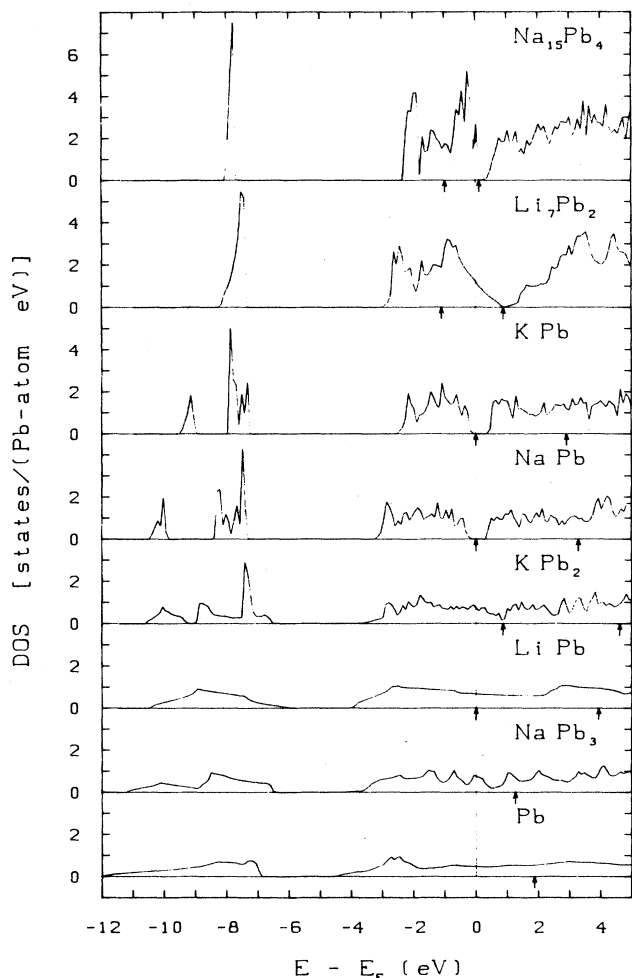


FIG. 12. Total densities of states of the seven alkali-metal-lead compounds and pure lead. The arrows indicate the middle and the top of the  $p$  band (i.e., the energies where the integrated densities of states reach five and eight states per Pb atom, respectively).

As the volume per lead atom is further decreased, this leads first to a percolation of the isolated Pb tetrahedra into a continuous network ( $KPb_2$ ). The strong inter-tetrahedra interaction causes the closing of the covalent gap. At still smaller volume per Pb atom the interaction becomes strong enough for the formation of a metallic Pb band, the alkali-metal bands being again above the Fermi level.

Thus, although their crystal structures and physical

properties are widely different, the bonding in the alkali-metal-lead compounds offers some unifying features. Despite the formation of an ionic gap separating cation and anion bands, and despite the large volume contraction, we are reluctant to classify the octet compounds as ionic, because the delocalization of the Pb states leads to very low net ionic charges and hence low ionicities. For the same reason we would not like to consider the semiconducting compounds as covalent, despite the origin of the energy gap in the bonding-antibonding splitting of the hybrid states derived from the lead  $p$  orbitals. Again the delocalized nature of these orbitals leads to bonding properties which are very different from a real covalent bond.

In all these compounds the cation  $s$  orbital always lies above the highest occupied anion orbital. Hence there is always some charge transfer even though a formal ionicity defined in terms of net charges within atomic spheres is low. If, following Robertson<sup>38,39</sup> we define a charge-transfer compound in terms of orbital energies this way, this provides a unifying concept for both the metallic and the semiconducting alkali-metal-lead compounds.

Finally we think that our results support the explanation for the high electrical resistivities found in the liquid alkali-metal-lead alloys at the equiatomic composition that has been put forward by van der Lugt and Geertsma.<sup>1</sup> In agreement with recent molecular-dynamics studies,<sup>14</sup> it is assumed that the Pb tetrahedra are preserved in the liquid phase. Since the alkali-metal atoms play only a minor role, the electronic structure of the liquid near to the equiatomic composition must be similar to that of the  $APb$  crystalline compounds (all isotypic to  $NaPb$ ). The gap between the bonding and antibonding Pb  $p$  states of the crystalline compound becomes a deep minimum in the liquid due to the disorder. At the equiatomic composition the Fermi level falls into this minimum causing high resistivities. As we move from K to Cs in the periodic system, the volume per lead atom in the  $APb$  compound or liquid increases. We have seen (Table IV and Fig. 12) that this results in a narrowing of the bands and a widening of the gap between the bonding and antibonding Pb  $p$  states. Thus the height of the resistivity peak increases in this series in qualitative agreement with the experimental results.<sup>1,8</sup>

#### ACKNOWLEDGMENTS

This work has been supported by the Jubiläumfonds der österreichischen Nationalbank under Projects No. 2991 and No. 3204.

\*Permanent address: Central Research Institute for Physics, P.O. Box 49, H-1525 Budapest, Hungary.

<sup>1</sup>W. van der Lugt and W. Geertsma, *Can. J. Phys.* **65**, 326 (1987).

<sup>2</sup>J. F. Smith and Z. Moser, *J. Nucl. Mater.* **59**, 158 (1976).

<sup>3</sup>M. Hansen and K. Anderko, *Constitution of Binary Alloys*, 2nd

ed. (McGraw-Hill, New York, 1958), p. 997.

<sup>4</sup>H. Schaefer, B. Eisenmann, and W. Müller, *Angew. Chem.* **85**, 742 (1973).

<sup>5</sup>H. Schaefer and B. Eisenmann, *Rev. Inorg. Chem.* **3**, 29 (1981).

<sup>6</sup>J. A. Meijer, W. Geertsma, and W. van der Lugt, *J. Phys. F* **15**, 899 (1985).

- <sup>7</sup>A. N. Kusnetzov, K. A. Chuntunov, and S. P. Yatsenko, *Russ. Metallurgy (Metally)* No. 5, 178 (1977) (English translation: Scientific Information Consultants, London).
- <sup>8</sup>J. A. Meijer, G. B. Vinke, and W. van der Lugt, *J. Phys. F* **16**, 845 (1986).
- <sup>9</sup>H. Ruppertsberg and H. Reiter, *J. Phys. F* **12**, 1311 (1982).
- <sup>10</sup>S. Tamaki, *Z. Phys. Chem. (Neue Folge)* **156**, 537 (1988).
- <sup>11</sup>H. T. J. Reijers (private communication).
- <sup>12</sup>H. T. J. Reijers, W. van der Lugt, and C. van Dijk, *Physica B+C* **144**, 404 (1987).
- <sup>13</sup>M.-L. Saboungi, R. Blomquist, K. J. Volin, and D. L. Price, *J. Chem. Phys.* **87**, 2278 (1987).
- <sup>14</sup>J. Hafner, *J. Phys. Condensed Matter* **1**, 1133 (1989).
- <sup>15</sup>R. Avci and C. P. Flynn, *Phys. Rev. B* **19**, 5967 (1979).
- <sup>16</sup>C. W. Bates, P. M. Th. van Attekum, G. K. Wertheim, K. W. West, and D. N. E. Buchanan, *Phys. Rev. B* **22**, 3968 (1980).
- <sup>17</sup>W. Geertsma, J. Dijkstra, and W. van der Lugt, *J. Phys. F* **14**, 1833 (1984); W. van der Lugt and W. Geertsma, *J. Non-Cryst. Solids* **61&62**, 187 (1984).
- <sup>18</sup>W. Geertsma, *J. Phys. C* **18**, 2461 (1985).
- <sup>19</sup>F. Springelkamp, R. A. de Groot, W. Geertsma, W. van der Lugt, and F. M. Mueller, *Phys. Rev. B* **32**, 2319 (1985).
- <sup>20</sup>A. R. Williams, J. Kübler, and C. D. Gelatt, *Phys. Rev. B* **19**, 6094 (1979).
- <sup>21</sup>J. Skriver, *The LMTO Method*, Vol. 41 of *Solid State Sciences Series* (Springer, Heidelberg, 1981).
- <sup>22</sup>O. K. Andersen, O. Jepsen, and D. Glötzel, in *Highlights of Condensed Matter Theory*, edited by F. Bassani, F. Fumi, and M. P. Tosi (North-Holland, Amsterdam, 1985).
- <sup>23</sup>U. von Barth, L. Hedin, and J. F. Janak, *Phys. Rev. B* **12**, 1257 (1975).
- <sup>24</sup>O. Jepsen and O. K. Andersen, *Solid State Commun.* **9**, 1763 (1971).
- <sup>25</sup>G. Lehman and M. Taut, *Phys. Status Solidi B* **54**, 469 (1972).
- <sup>26</sup>N. E. Christensen, *Phys. Rev. B* **30**, 5753 (1984).
- <sup>27</sup>P. Villars and N. E. Calvert, *Pearson's Handbook of Crystallographic Data for Intermetallic Phases* (American Metals Society, Metals Park, 1985).
- <sup>28</sup>R. E. Marsh and D. P. Shoemaker, *Acta Crystallogr.* **6**, 197 (1963).
- <sup>29</sup>I. F. Hewaidy, E. Busmann, and W. Klemm, *Z. Anorg. Allgem. Chem.* **328**, 283 (1964).
- <sup>30</sup>J. Hafner, *J. Phys. F* **15**, L43 (1985).
- <sup>31</sup>J. Witte and H. G. von Schering, *Z. Anorg. Allgem. Chem.* **327**, 260 (1964).
- <sup>32</sup>W. B. Pearson, *The Crystal Chemistry and Physics of Metals and Alloys* (Wiley, New York, 1972), p. 376.
- <sup>33</sup>R. R. Hart, M. B. Robin, and N. A. Kubler, *J. Chem. Phys.* **42**, 3631 (1965).
- <sup>34</sup>N. B. Goodman, L. Ley, and D. W. Bullett, *Phys. Rev. B* **27**, 7440 (1983).
- <sup>35</sup>J. A. Meijer, Ph.D. thesis, University of Groningen, 1988.
- <sup>36</sup>W. Jank and J. Hafner (unpublished).
- <sup>37</sup>N. E. Christensen, S. Satpathy, and Z. Pawlowska, *Phys. Rev. B* **34**, 5977 (1986).
- <sup>38</sup>J. Robertson, *Phys. Rev. B* **27**, 6322 (1983).
- <sup>39</sup>J. Robertson, *Adv. Phys.* **32**, 361 (1983).